EVALUATION OF FATIGUE CRACK GROWTH RETARDATION AND ARREST IN BIFURCATED CRACKS

Antonio Carlos de Oliveira Miranda[1]
Marco Antonio Meggiolaro[2]
Jaime Tupiassú Pinho de Castro[3]
Luiz Fernando Martha[4]

Abstract

Fatigue crack kinking and bifurcation are well-known phenomena capable of inducing significant growth retardation or even crack arrest. However, symmetrically bifurcated crack models available in the literature cannot account for the propagation behavior observed in practice. In this work, specialized Finite Element (FE) and life assessment software are used to predict the reduction in the propagation rates in asymmetrically bifurcated cracks. The crack path and the associated stress intensity factors (SIF) of asymmetrically bifurcated cracks are numerically obtained for several bifurcation angles. A companion life assessment program is used to estimate the number of delay cycles associated with crack bifurcation, allowing for a better understanding of the influence of crack deflection in the propagation life of structural components.

Keywords: fatigue, crack bifurcation, growth retardation.

58th ABM Annual Congress - July 2003, Rio de Janeiro, RJ, Brazil
[1]Civil Eng., Ph.D., Civil Engineering Dept., PUC-Rio
[2]Mechanical Eng., Ph.D., Visiting Professor of the Mechanical Eng. Dept., PUC-Rio
[3]Mechanical Eng., Ph.D., Professor of the Mechanical Eng. Dept., PUC-Rio
[4]Civil Eng., Ph.D., Professor of the Civil Engineering Dept., PUC-Rio

1. Introduction

It is a well known phenomenon that fatigue cracks can significantly deviate from their mode I growth direction due to the influence of overloads, generating crack kinking or branching (Fig. 1). Since the stress intensity factors (SIF) associated to deflected or branched fatigue cracks can be considerably smaller than that of a straight crack with the same projected length, such deviations can cause retardation or even arrest of crack growth.

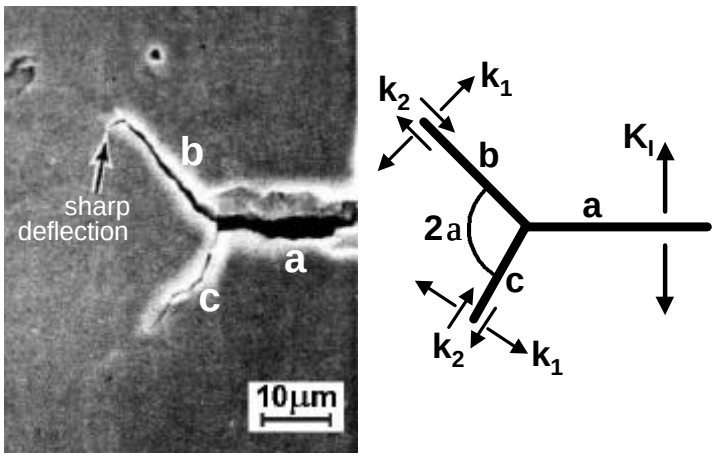

Figure 1 – Bifurcated crack geometry and associated nomenclature [1].

Analytical solutions [2] have been obtained for kinked and symmetrically branched cracks (**b** = **c** in Fig. 1), however there are very few results available for the real case of bifurcated cracks with different branch lengths (**b** > **c**). It is experimentally observed that very small differences between the branch lengths **b** and **c** are enough to cause the shorter branch to arrest as the larger one propagates, until reaching approximately its pre-overload SIF and growth rate. Therefore, although many branches can be developed along the main crack path, only the fastest branch continues to grow, while all others are brought to a stop due to the shielding caused by this fastest branch. This typical propagation behavior has been observed in many structural components, e.g. on a branched crack on an aircraft wheel rim made of 2014-T6 aluminum alloy [3].

However, the models available in the literature are symmetrical and cannot account for such effects. It is generally recognized that it is very difficult to develop accurate analytical solutions to the propagation behavior of branched cracks [4-6]. Therefore, numerical calculations provided e.g. by Finite Element (FE) software are usually the only means to predict such retardation effects.

To predict the path of a branched crack and to calculate the associated modes I and II stress intensity factors (SIF), an interactive graphical program named **Quebra2D** is used [7]. This program simulates two-dimensional fracture processes based on a finite-element (FE) self-adaptive mesh-generation strategy, using appropriate crack tip elements and crack increment criteria. It has been validated through experiments on several modified CT specimens and from comparisons with analytical solutions for kinked cracks.

The crack path and associated SIF are then exported to **ViDa**, a general-purpose fatigue design program developed to predict both initiation and propagation fatigue lives under variable loading by all classical design methods [8]. In particular, its crack propagation module accepts any stress-intensity factor expression,

including the ones generated by other FE software. This companion life assessment program is used to estimate the number of delay cycles associated with crack bifurcation. In the next sections, these two pieces of software are used to calculate the propagation behavior of bifurcated (branched) cracks.

2. Finite Element Software Description

The **Quebra2D** program simulates two-dimensional fracture processes based on a Finite-Element (FE) self-adaptive mesh-generation strategy, using appropriate crack tip elements and crack increment criteria [7]. The adaptive FE analyses are coupled with modern and efficient automatic remeshing schemes. The meshing algorithm especially developed for **Quebra2D** works both for regions without cracks and for regions with one or multiple cracks, which may be either embedded or surface breaking. The 2D algorithm has been designed to meet four specific requirements, as follows. First, the algorithm should produce well-shaped elements, avoiding elements with poor aspect ratio. Second, the generated mesh should conform to the specified discretization of the region boundary. Third, the algorithm should shift smoothly between regions with elements of highly varying size, because in crack analysis it is not uncommon for the elements near the crack tip to be two orders of magnitude smaller than the other elements. And fourth, the algorithm should have specific capabilities for modeling cracks, which are usually idealized without volume, i.e. the surfaces representing the two sides of a crack face are distinct, but geometrically coincident. This means that nodes on opposite sides of crack faces may have identical coordinates, and the algorithm must be able to discriminate between the nodes and to select the one on the proper crack side.

In the **Quebra2D** program, three methods can be chosen to compute the stress intensity factors along the (generally curved) crack path: the displacement correlation technique, the potential energy release rate computed by means of a modified crack-closure integral technique, and the J-integral computed by means of the equivalent domain integral (EDI) together with a mode decomposition scheme [7]. The EDI method replaces the J-integral along a contour by another one over a finite size domain, using the divergence theorem, which is more convenient for FE analysis. Since Bittencourt et al. [9] showed that for sufficiently refined FE meshes all three methods predict essentially the same results, only the EDI method is considered in the calculations presented here.

To calculate the propagation path, other three criteria can be used for the numerical computation of the crack incremental growth direction in the linear-elastic regime: the maximum circumferential stress ($\sigma_{\theta max}$), the maximum potential energy release rate ($G_{\theta max}$), and the minimum strain energy density ($S_{\theta min}$) [7]. Bittencourt et al. [9] have also shown that if the crack orientation is allowed to change in automatic fracture simulation, these three criteria basically provide the same numerical results.

3. Life Assessment Program Description

The purpose of the **ViDa** program is to automate, in a friendly environment, all calculations required to predict fatigue life under variable amplitude loading by means of the local approach [8]. It includes all necessary tools to perform the predictions, such as an intuitive and friendly graphical interface in six languages; intelligent databases for stress concentration and intensity factors, crack propagation models, material properties, and more; traditional and sequential rain-flow counters; graphical output for all computed results, including elastic-plastic hysteresis loops and 2D crack fronts; automatic adjustment of crack initiation and propagation

experimental data; an equation interpreter, etc. Crack growth can be calculated considering any propagation model and any **DK** expression that can be typed in (making it an ideal companion to the **Quebra2D** software, which can be used to generate the **DK(a)** expression if it is not available in the database).

The propagation is calculated at each load event. The calculations are automatically stopped if during the loading it detects that: (i) the maximum SIF reaches the fracture toughness; (ii) the crack reaches its maximum specified size; (iii) the stress in the residual ligament reaches the rupture strength of the material; (iv) the crack propagation rate reaches 0.1 mm/cycle (above this rate the problem is fracturing, not fatigue cracking); or (v) one of the borders of the specimen is reached by the crack front, in the surface crack propagation case. In this way, the calculated values can be used with the guarantee that the limit of validity of the mathematical models is never exceeded.

4. Crack Bifurcation Predictions

In this section, a standard CT specimen is FE modeled using **Quebra2D** with width **w = 32.0mm**, crack length **a = 14.9mm**, and crack branch lengths **c = 10mm** and **b = 10** or **20mm**. The modes I and II SIF $\mathbf{k_1}$ and $\mathbf{k_2}$ of each crack branch are obtained considering bifurcation angles **2a** between 30° and 180° (see Fig. 1). Note that typical overload-induced bifurcated cracks can have initial branch lengths between 10 and 100μm, with **2a** varying between 30° (for very brittle materials such as glass) and 180° (in the vicinity of the interface of a bi-material composite, when a crack propagates from the weak to the strong material [10]).

Figure 2 shows the FE results for the SIF $\mathbf{k_1}$ and $\mathbf{k_2}$ (normalized by the mode I SIF $\mathbf{K_I}$ of the straight crack) of symmetrically and asymmetrically bifurcated cracks. There is a marked increase in the $\mathbf{k'_1}$ and $\mathbf{k'_2}$ SIF for the larger branch (and decrease in the $\mathbf{k''_1}$ and $\mathbf{k''_2}$ of the shorter one), if compared to the symmetrically branched solutions. As the length difference between both branches increases, it is expected that the propagation rate of the shorter one is reduced until it arrests, after which the larger branch will dominate. This shielding effect of the longer branch over the shorter one is larger for small bifurcation angles, typically below 120°, see Fig. 2.

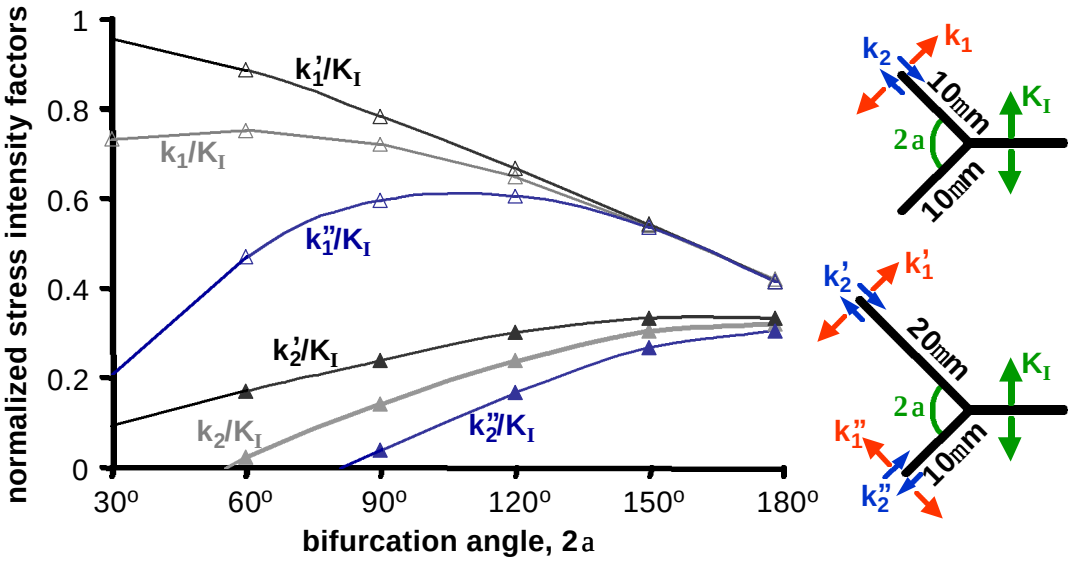

Figure 2 – Stress intensity factors for symmetrically and asymmetrically bifurcated cracks.

For large values of **2a**, the shielding effect is much smaller, as it would be expected since the branch tips would be further apart. Therefore, for larger bifurcation angles the shorter branch is expected to take a longer time to arrest, prolonging the retardation effect.

However, it must be pointed out that these FE results might have some limitations, because such small bifurcations can be of a size comparable to the scale of local plasticity (e.g. the plastic zone size) or microstructural features (e.g. grain size). Moreover, possible closure and environmental effects should be considered when comparing the bifurcation model predictions with measured crack growth rates [2].

5. Propagation of Branched Cracks

The growth of branched cracks is studied in the **Quebra2D** program using the same CT specimen described above, considering initial branch lengths **b = 11mm** and **c = 10mm** (see Fig. 1). The bifurcation angles **2a** in this study vary between **60°** and **150°**.

A fixed crack growth step of **Db = 3mm** is considered for the propagation of the longer branch **b**, calculated in the direction defined by the $\sigma_{\theta max}$ criterion (which is the criterion adopted in this simulation, due to its simplicity and to the availability of closed form solutions). However, due to the differences in the crack growth rate, a smaller growth step is expected for the shorter branch. This smaller step is obtained assuming a crack propagation law that models the first two growth regimes,

$$\frac{da}{dN} = A \times (\Delta K - \Delta K_{th})^m \qquad (1)$$

where **A** and **m** are material constants and ΔK_{th} is the propagation threshold. If ΔK and $\Delta K'$ are respectively the stress intensity ranges of the longer and shorter branches, then the growth step **Dc** of the shorter branch **c** should be

$$\Delta c = \Delta b \times \left(\frac{\Delta K' - \Delta K_{th}}{\Delta K - \Delta K_{th}}\right)^m \qquad (2)$$

Interestingly, the ratio between the propagation rates of the two branches is independent of the material constant **A**. In this analysis, ΔK_{th} and the exponent **m** are assumed to be respectively **10MPa√m** and **3.0**, which are representative values for steels at low **R** ratios.

It must be noted however that linear-elastic FE calculations can only lead to accurate solutions if the lengths of the crack branches (**b** and **c** in Fig. 1) are significantly larger than the size scale of both the microstructure and the near-tip plastic (or process) zone. But as the crack branches grow further, the FE method can give a reasonable estimate of their behavior, in special for brittle or semi-brittle materials with small process zones. In addition, the growth of branched cracks is typically transgranular, as verified from optical microscope observations performed by Shi [11], which is one of the requirements to allow for the simulation of fatigue behavior in isotropic linear-elastic regime.

Figure 3 shows the mode I SIF k_1 at the tip of each crack branch (normalized by the mode I SIF K_I of a straight crack) as a function of the length **b** of the longer branch, measured along the propagation path. Because of the different crack branch lengths, the SIF at the larger is much higher than that at the shorter branch. Assuming k_1 to be the crack driving force, it can be seen from Fig. 3 that the longer

branch reaches its minimum propagation rate right after the bifurcation occurs, returning to its pre-overload rate as the crack tip advances away from the influence of the shorter branch. Also, the mode I SIF of the shorter branch is progressively reduced due to shielding effects, resulting in crack arrest as the propagation threshold ΔK_{th} is reached. Note that even small differences between the branch lengths (such as the **1mm** assumed here) are sufficient to cause subsequent arrest of the shorter branch. In addition, the retardation effect lasts longer for larger bifurcation angles, not only because the associated mode I SIF is smaller, but also because the shielding effect is weaker since both branch tips are further apart, delaying the arrest of the shorter one.

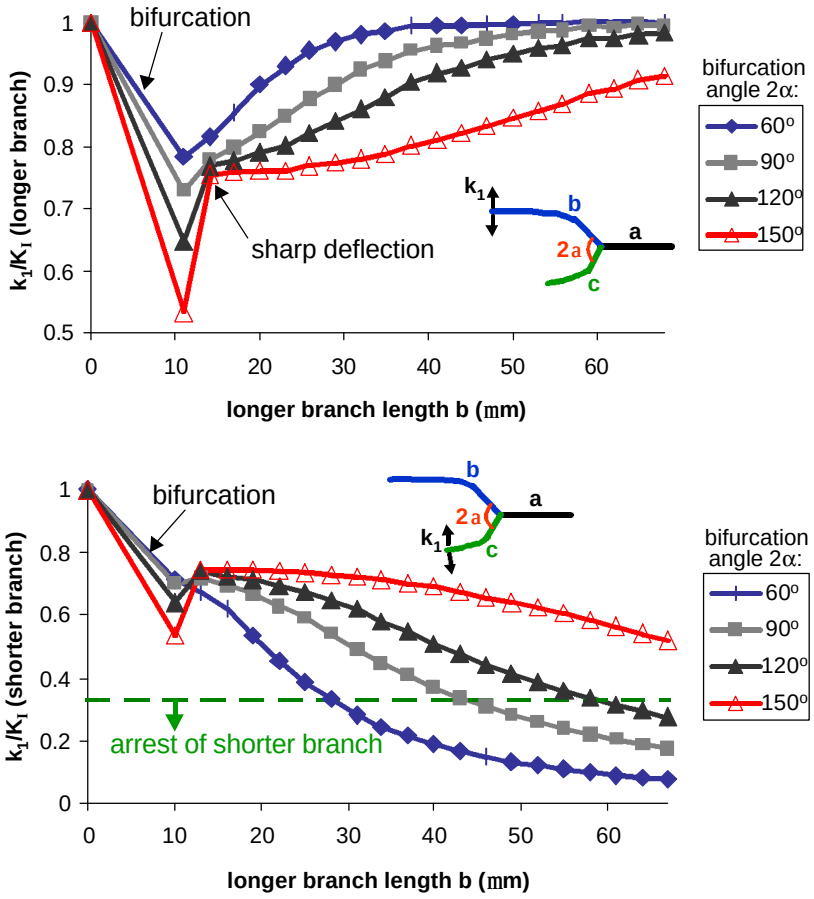

Figure 3 – Normalized mode I stress intensity factors for the longer (top) and shorter (bottom) branches of a bifurcated crack during its propagation.

Another interesting conclusion is that the initial propagation direction of the longer branch is always between 25° and 30° (with respect to the pre-overload growth direction), independently of the considered bifurcation angle **2a**. Therefore, for larger values of **2a**, a sharp deflection can be clearly noted in the beginning of the propagation. This deflection has been experimentally confirmed by Lankford and Davidson [1], who carried out overload fatigue crack tests on a 6061-T6 aluminum alloy in a scanning electron microscope using a special in-situ servo-controlled hydraulic loading stage, obtaining growth retardation caused by crack bifurcation. They have found that the bifurcated crack would grow only a short distance in the same direction of the overload-induced bifurcation, before a sharp deflection in the crack path would occur, see Fig. 1. This deflection causes a sudden increase in $\mathbf{k_1}$

almost immediately after the propagation begins (Fig. 3), resulting in a significantly smaller retardation effect if compared to simplistic predictions based on symmetrically branched crack solutions found in the literature. However, if the SIF of both branches is below ΔK_{th}, then the entire crack arrests and therefore no sharp deflection has the chance to develop.

Figure 4 shows the contour plots of the stress in the load direction axis and propagation results for a bifurcated crack with angle $2\alpha = 150^{o}$, obtained from the FE analysis. In this figure, the deformations are highly amplified to better visualize the crack path. Note that the crack path deviates from the original branch angles, deflecting from $\pm 75^{o}$ to approximately $\pm 28^{o}$. In addition, the originally shorter branch arrests after propagating to (only) **39mm**, while the longer branch returns to the pre-overload growth direction and SIF (even though the subsequent crack growth plane may be offset from the pre-overload one, see Fig. 4).

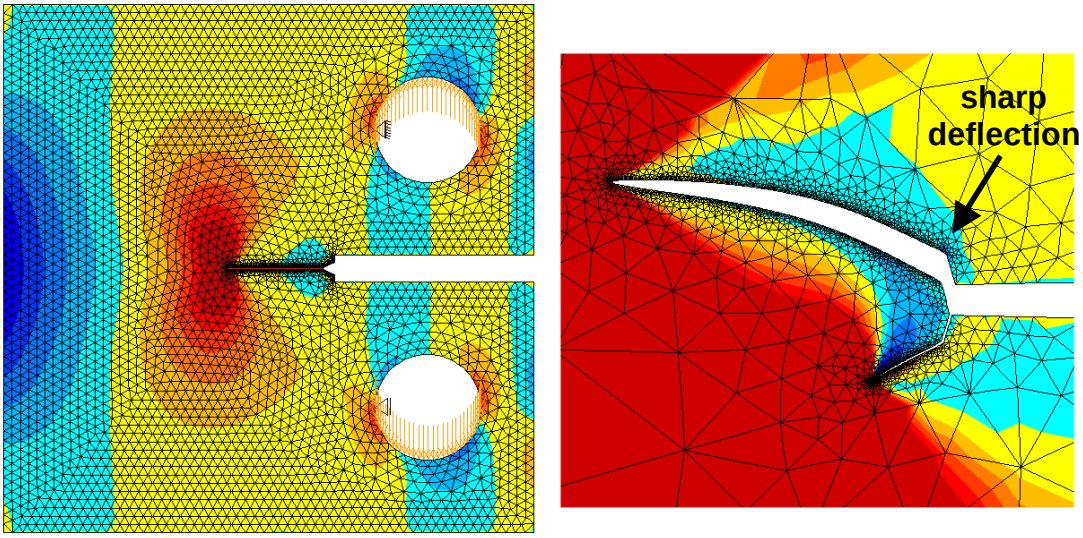

Figure 4 – Propagation simulation of a bifurcated crack on a CT specimen (left), with a close-up of the two original **11mm** and **10mm** branches with angle $2\alpha = 150^{o}$ (right).

A qualitative validation of the predicted bifurcated crack growth behavior is performed using 40mm-wide 8mm-thick compact tension C(T) test specimens, made of SAE 1020 steel with yield strength S_Y **= 285MPa**, ultimate strength S_U **= 491MPa**, Young modulus **E = 205GPa**, and reduction in area **RA = 54%**, measured according to the ASTM E 8M-99 standard, and with the analyzed weight percent composition given in Table 1. The tests are performed at frequencies between 20 and 30 Hz in a 250kN computer-controlled servo-hydraulic testing machine. The crack length was measured following ASTM E 647-99 procedures. Figure 5 shows the measured paths of a branched crack induced by a 70% overload. As predicted, the shorter branch tends to arrest as the longer one continues to grow, returning to its original propagation direction.

The same crack growth behavior is observed on Eccentrically-loaded Single Edge Crack Tension specimens ESE(T) made of SAE 4340 steel with S_Y **= 377MPa**, S_U **=** 660MPa, **E = 205GPa**, and **RA = 52.7%**, and with the analyzed weight percent composition given in Table 2. The specimen dimensions are given in Fig. 6. The tests are performed under the same conditions as those on the SAE 1020 specimens. Figure 7 shows the measured paths of a branched crack induced by a **50%** overload when the crack length was **a = 25.55 mm**.

Table 1 - Chemical composition of the tested SAE 1020 steel (weight %)

C	Mn	Si	Cu	Ni	Cr	S	P	Mo	Nb	Ti	Fe
0.19	0.46	0.14	0.11	0.052	0.045	0.05	0.04	0.007	0.002	0.002	balance

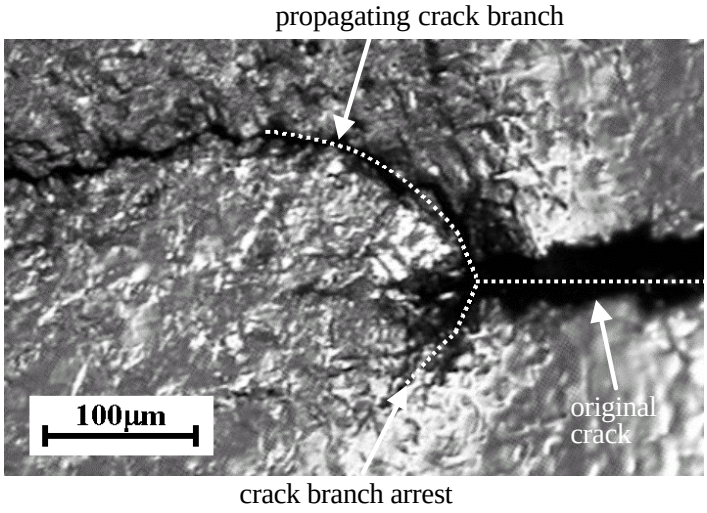

Figure 5 – Crack branching on an SAE 1020 C(T) specimen.

Table 2 - Chemical composition of the tested SAE 4340 steel (weight %)

C	Mn	Si	Ni	Cr	S	P	Mo	Fe
0.37	0.56	0.14	1.53	0.64	0.04	0.035	0.18	balance

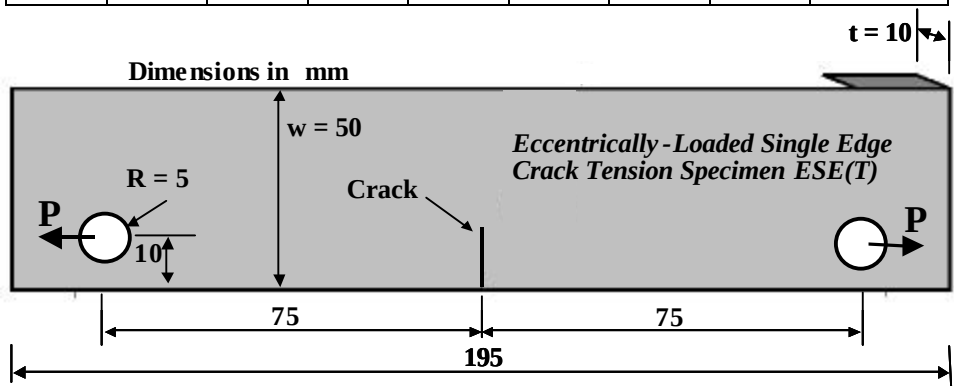

Figure 6 – Geometry of the tested ESE(T) specimen.

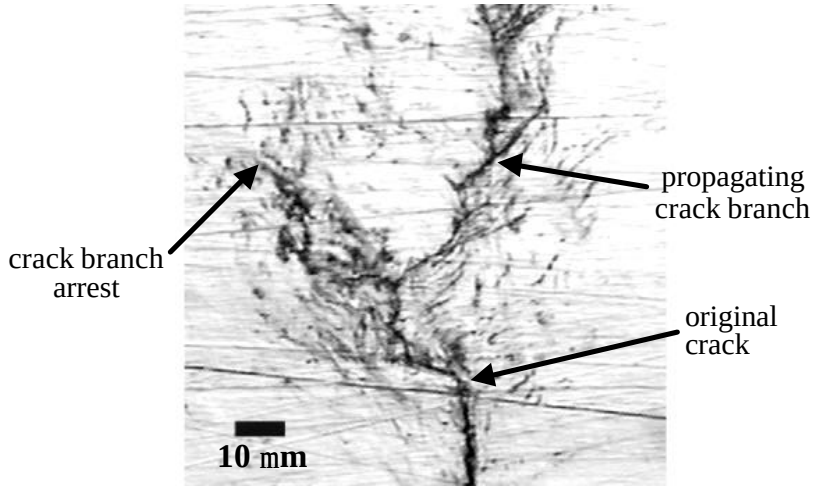

Figure 7 – Crack branching on an SAE 4340 ESE(T) specimen.

6. Life Assessment of Branched Cracks

To estimate the number of delay cycles associated with crack bifurcation, the crack path and SIF values calculated using **Quebra2D** are exported to the **ViDa** program, where the crack propagation equation can be easily integrated.

Ideally, it would be desirable to fit a bifurcation function $\mathbf{f_b}$ for the longer branch, defined as the ratio between the mode I SIF $\mathbf{k_1}$ at the tip of the longer crack branch and the mode I SIF $\mathbf{K_I}$ of the original straight crack, which is plotted in Fig. 3. However, it has been identified in crack propagation simulations that $\mathbf{f_b}$ is not only a function of the longer branch length **b**, but it also depends on the bifurcation geometry through the initial lengths of the crack branches $\mathbf{b_0}$ and $\mathbf{c_0}$, and the bifurcation angle $\mathbf{2}\alpha$. In addition, as equation (2) plays a large role in the crack path simulations, it can be concluded that $\mathbf{f_b}$ is also a function of the exponent **m** of the **da/dN** equation, the propagation threshold $\Delta\mathbf{K_{th}}$, and the stress intensity range $\Delta\mathbf{K_I}$ of the original straight crack, therefore

$$\frac{\mathbf{k_1}}{\mathbf{K_I}} = \mathbf{f_b}(\mathbf{b},\ \mathbf{b_0},\ \mathbf{c_0},\ \mathbf{2}\alpha,\ \mathbf{m},\ \Delta\mathbf{K_{th}},\ \Delta\mathbf{K_I}) \tag{3}$$

Such bifurcation function $\mathbf{f_b}$ would be, at least in theory, applicable to any bifurcated crack in any specimen, provided that the crack branches are small if compared to the specimen geometry and that the propagation behavior of the material can be described using equation (1). However, to obtain such an universal bifurcation function, it would be necessary to perform extensive FE calculations varying all the six independent parameters.

In this section, $\mathbf{f_b}$ is evaluated in **Quebra2D** and a fifth-order polynomial is fitted as a function of the longer branch length **b** (in mm), considering initial branch lengths $\mathbf{b_0 = 11\mu m}$ and $\mathbf{c_0 = 10\mu m}$, bifurcation angle $\mathbf{2}\alpha\ \mathbf{= 150^o}$, crack growth constants $\mathbf{A = 3.0\times10^{-10}\ m/cycle}$ and **m = 3.0**, $\mathbf{\Delta K_{th} = 10MPa\sqrt{m}}$, and $\mathbf{\Delta K_I = 30MPa\sqrt{m}}$, resulting in

$$\begin{aligned}\mathbf{f_b}(\mathbf{b,\ 11\mu m,\ 10\mu m,\ 150^o,\ 3.0,\ 10MPa\sqrt{m},\ 30MPa\sqrt{m}}) = \\ = \mathbf{0.75 - 0.94b + 52b^2 + 700b^3 - 15400b^4 + 63500b^5}\end{aligned} \tag{4}$$

This particular case of the $\mathbf{f_b}$ function is only valid for the specified parameters and **b** values between $\mathbf{b_0}$ (**= 11μm = 0.011mm**) and **0.120mm**, after which $\mathbf{f_b}$ approaches 1.0 and the bifurcation effect becomes negligible.

The $\mathbf{f_b}$ expression is then exported to the **ViDa** program to estimate the number of cycles required to grow the longer branch **b** from **11** to **120μm**, considering a baseline $\Delta\mathbf{K_I}$ of $\mathbf{30MPa\sqrt{m}}$ and a material that follows

$$\frac{\mathbf{da}}{\mathbf{dN}} = \mathbf{3.0\times10^{-10}}(\Delta\mathbf{K - 10})^{\mathbf{3.0}} \tag{5}$$

It is found that the reduction in the SIF caused by the bifurcation increases the required number of cycles from 45 to 105, therefore resulting in approximately 60 delay cycles. This low delay is largely due to the considered baseline $\Delta\mathbf{K_I}$ being much larger than $\Delta\mathbf{K_{th}}$. In fact, extrapolations of the $\mathbf{f_b}$ function considering a baseline $\Delta\mathbf{K_I}$ value of $\mathbf{14MPa\sqrt{m}}$ resulted in over 720000 delay cycles, because the reduction in the SIF of the longer branch would almost cause crack arrest in this case.

7. Conclusions

In this work, a specialized FE program was used to calculate the propagation path of bifurcated cracks, which can cause crack retardation or even arrest. It is found that crack deflection processes alone can significantly reduce the stress intensity factors (SIF) and therefore the propagation rates, leading to crack retardation or even arrest. In particular, the ratio between the bifurcated and the pre-overload mode I SIF can be as low as 0.4. It was shown that asymmetrically bifurcated cracks have a very different behavior than symmetrical ones, causing arrest of the shorter branch as the longer one returns to the pre-overload propagation conditions. Also, very small differences between the lengths of the bifurcated branches are sufficient to induce a much larger SIF and thus crack propagation of the longer branch. Life assessment calculations were performed using a local approach program to estimate the number of delay cycles caused by crack bifurcation, allowing for a better understanding of the influence of crack deflection in the propagation life of structural components. From these results, it is found that crack bifurcation may provide an alternate mechanistic explanation for overload-induced crack retardation, in special to explain retardation under high **R** ratios, since no crack closure would be detected in these cases.

References

[1] LANKFORD, J.; DAVIDSON, D.L. The effect of overloads upon fatigue crack tip opening displacement and crack tip opening/closing loads in aluminum alloys. In **Advances in Fracture Research**, Pergamon Press, v. 2, p. 899-906, 1981.

[2] SURESH, S. Crack deflection: implications for the growth of long and short fatigue cracks. **Metallurgical Transactions**, v. 14A, p. 2375-85, 1983.

[3] KOSEC, B.; KOVACIC, G.; KOSEC, L. Fatigue cracking of an aircraft wheel. **Engineering Failure Analysis**, v. 9, p. 603-9, 2002.

[4] SURESH, S. Micromechanisms of fatigue crack growth retardation following overloads. **Engineering Fracture Mechanics**, v. 18, n. 3, p. 577-93, 1983.

[5] SURESH, S. **Fatigue of materials**. Cambridge University Press, 1998. 679p.

[6] SEELIG, T.; GROSS, D. On the interaction and branching of fast running cracks - a numerical investigation. **Journal of the Mechanics and Physics of Solids**, v. 47, p. 935-52, 1999.

[7] MIRANDA, A. C. O.; MEGGIOLARO, M. A.; CASTRO, J. T. P.; MARTHA, L. F.; BITTENCOURT, T.N. Fatigue crack propagation under complex loading in arbitrary 2D geometries. In: Braun AA, McKeighan PC, Lohr RD, editors. **Applications of Automation Technology in Fatigue and Fracture Testing and Analysis, ASTM STP 1411(4)**, p. 120-46, 2002.

[8] MEGGIOLARO, M. A.; CASTRO, J. T. P. ViDa 98 - Danômetro Visual para Automatizar o Projeto à Fadiga sob Carregamentos Complexos. **J. Brazilian Society of Mechanical Sciences (RBCM)**, v. 20, n. 4, p. 666-685, 1998.

[9] BITTENCOURT, T. N.; WAWRZYNEK, P. A.; INGRAFFEA, A. R.; SOUSA, J. L. A. Quasi-automatic simulation of crack propagation for 2D LEFM Problems. **Eng. Fracture Mechanics**, v. 55, p. 321-34, 1996.

[10] PIPPAN, R.; FLECHSIG, K.; RIEMELMOSER, F. O. Fatigue crack propagation behavior in the vicinity of an interface between materials with different yield stresses. **Materials Science and Engineering**, v. A283, p. 225-33, 2000.

[11] SHI, H. J.; NIU, L. S.; MESMACQUE, G.; WANG, Z.G. Branched crack growth behavior of mixed-mode fatigue for an austenitic 304L steel. **International Journal of Fatigue**, v. 22, p. 457-65, 2000.